CO_2-switchable multicompartment micelles with segregated corona

Hanbin Liu,[ae] Ying Zhao,[c] Cécile A. Dreiss[d] and Yujun Feng*[ab]

[a] Chengdu Institute of Organic Chemistry, Chinese Academy of Sciences, Chengdu 610041, P. R. China

[b] Polymer Research Institute, State Key Laboratory of Polymer Materials Engineering, Sichuan University, Chengdu 610065, P. R. China
E-mail: yjfeng@scu.edu.cn

[c] Institute of Nano-Photonics, School of Physics and Materials Engineering, Dalian Nationalities University, Dalian 116600, P. R. China

[d] Institute of Pharmaceutical Science, 150 Stamford Street, King's College London, UK SE1 9NH

[e] University of the Chinese Academy of Sciences, Beijing 100049, P. R. China

1. Materials

2-(Diethylamino)ethyl methacrylate (DEAEMA, Aldrich, 99%) and 2,2,3,4,4,4-Hexafluorobutyl methacrylate (HFBMA, Aldrich, 99%) were passed through an activated basic alumina column to remove the inhibitors prior to use. 4,4-Azobis(4-cyanopentanoic acid) (ACPA), 4-(dimethylamino)pyridine (DMAP), N-(3-Dimethylaminopropyl)-N′-ethylcarbodiimide hydrochloride crystalline (EDAC), poly(ethylene glycol) methyl ether (mPEG-5000, M_n ~5,000 g·mol^{-1}), 2,3,4,5,6-pentafluoroaniline and Rhodamine B, were purchased from Sigma–Aldrich and used as received. All other reagents were obtained from Shanghai Chemical Reagent Co., Ltd. and used without further treatment unless otherwise specified. The deionized water (conductivity, κ=12.8 μS·cm^{-1}) used in the experiments was treated by an ultrapure water purification system (Chengdu Ultrapure Technology Co., Ltd., China).

The chain transfer agent (CTA) for reversible addition-fragmentation chain transfer (RAFT) polymerization, 4-cyano-4-thiothiopropylsulfanylpentanoic acid (CTPPA), was synthesised according to a previously reported procedure.[1,2]

2. Characterization

Nuclear Magnetic Resonance Spectroscopy (NMR). ^{1}H NMR spectra were recorded at 25 °C on a Bruker AV300 NMR spectrometer (300 MHz). The chemical shifts (δ) were reported in parts per million (ppm) with reference to the internal standard protons of tetramethylsilane (TMS).

Gel Permeation Chromatography (GPC). The molecular weight and the molecular weight distribution of the polymers were determined by a HLC-8320 gel permeation chromatography system (TOSOH, Japan) equipped with TSK gel super HZM-M 6.0×150 mm and TSK gel SuperHZ3000 6.0×150 mm chromatographic column and refractive index detector. THF was used as the eluent at a flow rate of 0.6 $mL \cdot min^{-1}$ at 40 ºC. Monodisperse polystyrene was used as the standard to generate the calibration curve.

Transmission Electron Microscopy (TEM). TEM observations were performed on a Tecnai G2 F20 (FEI Co.) field emission transmission electron microscope operated at an acceleration voltage of 200 kV. The specimens were prepared by placing one drop of the polymer aqueous solution (1.0 $g \cdot L^{-1}$) onto formvar-coated copper grids. Excessive solvent was instantly absorbed by filter paper. Afterwards, the samples were dipped into the phosphotungstic acid solution (0.2 wt%) and left for approximately 30 seconds to stain the micelles. For RuO_4 staining, the samples were dried on the copper grid for several hours and then exposed to RuO_4 vapor for 8 min before visualization.

Scanning Electron Microscopy (SEM). SEM measurements were conducted on a JSM-7500F (JEOL, Japan) field emission scanning electron microscope. The sample for SEM observation was prepared by depositing several drops of the solution (1 $g \cdot L^{-1}$) after treatment with CO_2 onto the surface of a freshly-cleaved mica substrate, and then dried in a lyophilizer.

Atomic Force Microscopy (AFM). AFM images were taken in tapping-mode with an atomic force microscope (AFM, MFP-3D-BIO, Asylum Research, USA), under ambient conditions in air. The diameter of the assemblies was generated from the sectional analysis with the software Igor Pro 6.04. To prepare the samples, a drop of the micellar solution (1.0 $g \cdot L^{-1}$) was placed onto a freshly-cleaved mica substrate, and then dried in a lyophilizer.

Cryogenic Transmission Electron Microscopy (cryo-TEM). Cryo-TEM observations were performed on a JEM2010 cryo-microscope (JEOL, Japan) at an acceleration voltage of 200 kV. A drop of the micelle solution was deposited on a carbon-coated copper grid. The excess solution was absorbed with filter paper, and the specimen was rapidly plunged into liquid ethane and transferred to liquid nitrogen where it was kept until use. The images were recorded digitally with a charge-coupled device camera (Gatan 832) under low-dose conditions with an under-focus of approximately 3μm.

Dynamic Light Scattering (DLS). A laser light scattering spectrometer (ALV/DLS/SLS-5022F) equipped with a multi-tau digital time correlator (ALV5000) and a 22 mW He-Ne laser (λ_0 = 632 nm) as the light source was used to detect the hydrodynamic radius R_h. In the experiments, scattered light was collected at a fixed angle of 90º for a duration of ~10 min. The average radius $\langle R_h \rangle$ and particle size distributions $\langle f_h \rangle$ were computed using the cumulants analysis and CONTIN routines.

Differential Scanning Calorimetry (DSC). The thermal behaviour of the block copolymers was measured by a Q200 Differential Scanning Calorimeter (TA Instruments, USA) from –

80 to 100 °C at a heating rate of 10 °C·min^{-1} under nitrogen atmosphere.

3. Synthesis

The general synthesis protocol of the triblock copolymer is given in Scheme S1.

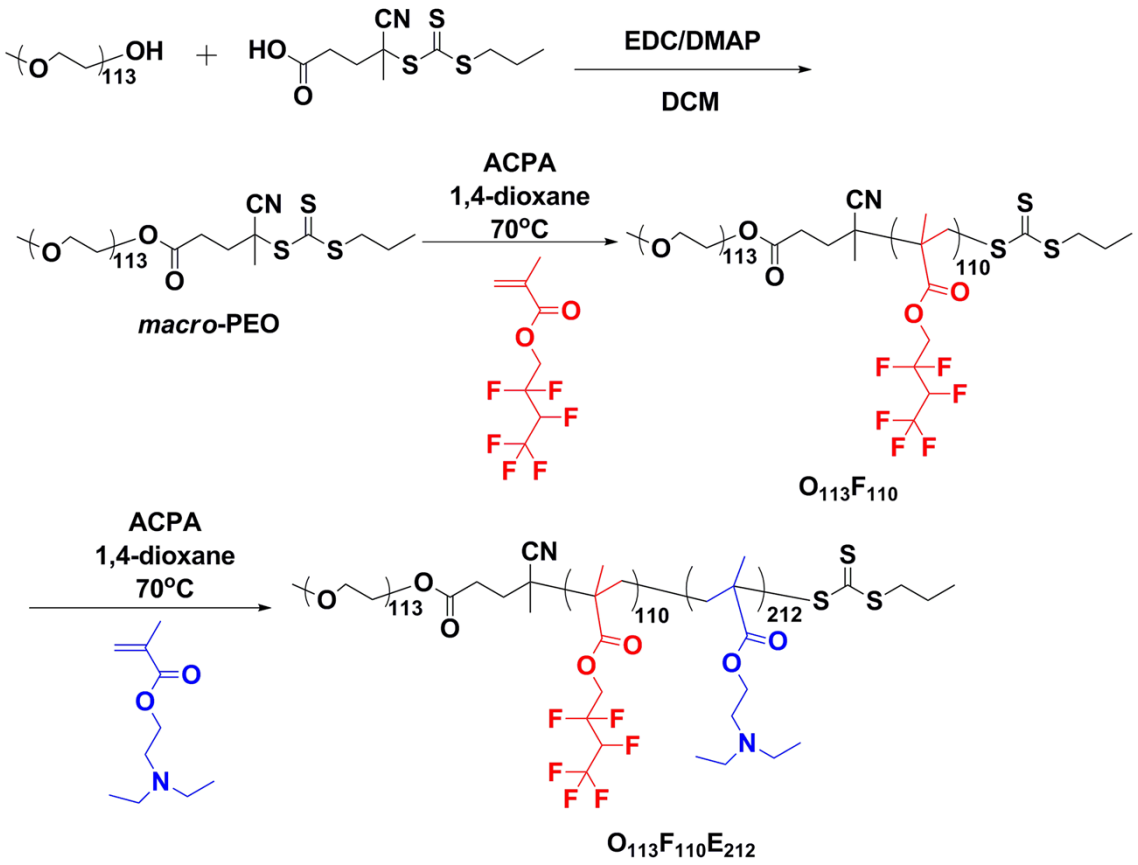

Scheme S1. Synthesis route of the triblock copolymer.

1) Synthesis of the Macromolecular RAFT agent *macro*–PEO

The macro-PEO is synthesized by an esterification reaction catalyzed by EDC and DMAP. Dichloromethane (DCM) was dried with CaH_2 and then refluxed to serve as a solvent for this reaction. A typical procedure is as follows: the chain transfer agent CTPPA (0.554 g, 2.0 mmol), mPEG-5000 (5.003 g, 1.0 mmol), EDAC (0.767 g, 4.0 mmol), and DMAP (0.244 g, 2.0 mmol) were dissolved in 50 mL dried DCM, then added into a 100-mL round bottom flask equipped with a magnetic bar, stirring for 48 h at room temperature after deoxygenating by bubbling Ar for 15 min. The reaction mixture was concentrated and precipitated in –72 °C *n*-hexane (in bath of acetone and dry ice mixture) three times, and then washed with diethyl ether for three times. Finally, a yellow powder was obtained after lyophilisation (4.8 g, yield: 96%). ^{1}H NMR (δ, ppm, $CDCl_3$; Figure S1): 3.62 (–C**H**$_2$C**H**$_2$O–), 3.36 (–OC**H**$_3$, –SC**H**$_2$–), 2.38–2.71 (–OOCC**H**$_2$C**H**$_2$–), 1.85 (–C(C**H**$_3$)(CN)–), 1.67–1.85 (–SCH$_2$C**H**$_2$CH$_3$), 0.97–1.02 (–SCH$_2$CH$_2$C**H**$_3$). $M_{n,GPC}$=6952 g·mol^{-1}, $M_{w,GPC}$=7111 g·mol^{-1}, M_w/M_n=1.02 (Figure S5).

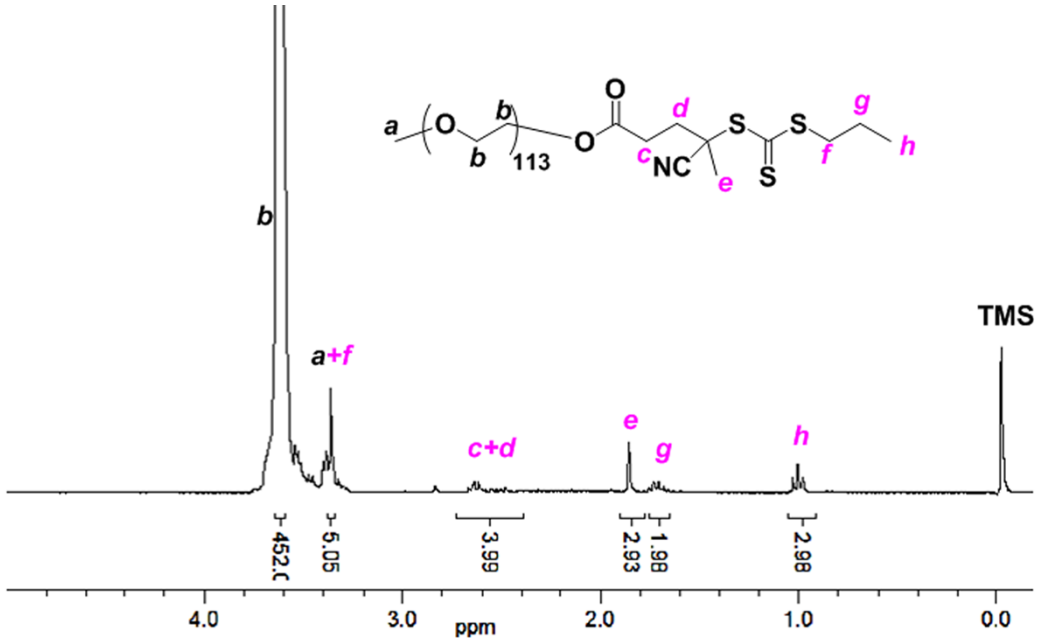

Figure S1. ^{1}H NMR spectrum of *macro*–PEO_{113} in $CDCl_3$.

2) Synthesis of the diblock copolymer PEO-*b*-PHFBMA

Using the macro-PEO as a macromolecular RAFT agent, the diblock copolymer PEO-*b*-PHFBMA (OF) was synthesized as follows: the macro-PEO (1.001 g, 0.19 mmol), the initiator ACPA (0.011 g, 0.038 mmol), the monomers HFBMA (8.552 g, 34 mmol) and 5 mL of 1,4-dioxane were added into a reaction tube equipped with a magnetic bar, followed by three freeze-pump-thaw cycles. The mixture was reacted at 70 °C accompanied by magnetic stirring for 48 h. The polymerization was stopped by freezing the reaction tube into liquid nitrogen for more than 5 minutes. Then the product was obtained after precipitation into *n*-hexane and lyophilized in a freezing dryer (yield: 8.0 g; conversion: 84%). ^{19}F NMR (δ, ppm, $CDCl_3$; Figure S4): –74 (–C**F**$_3$), –114 (–C**F**$_2$–), –120 (–C**F**–); ^{1}H NMR (δ, ppm, $CDCl_3$; Figure S2): 4.72–5.08 (–C**H**FCF_3), 4.03–4.61 (–COOC**H**$_2$CF_2–), 3.64 (–C**H**$_2$C**H**$_2$O–), 3.37 (–OC**H**$_3$), 3.24 (–SC**H**$_2$–), 2.82 (–OOCC**H**$_2$C**H**$_2$–) 1.58–1.82 (–C(C**H**$_3$)(CN)–, –CH_2C**H**$_3$CH_2–, –SCH_2C**H**$_2$CH_3), 0.82–1.18 (–C**H**$_2$CH_3C**H**$_2$–, –SCH_2CH_2C**H**$_3$). From the peak area ratio of PEO_{113} (peak *b* in the bottom curve of Figure S2) and the "F" block (peak *i* or *h* in the bottom curve of Figure S2), it is easy to calculate the polymerisation degree of HFBMA, for which we obtained $DP_{HFBMA,NMR}$=110. The molecular weight of the diblock copolymer $O_{113}F_{110}$ can be calculated as: $M_{n,NMR}$= 5276+250×110=3.3×10^4 g·mol^{-1}; $M_{n,GPC}$=2.25×10^4 g·mol^{-1}, $M_{w,GPC}$=3.03×10^4 g·mol^{-1}, M_w/M_n=1.35 (Figure S5).

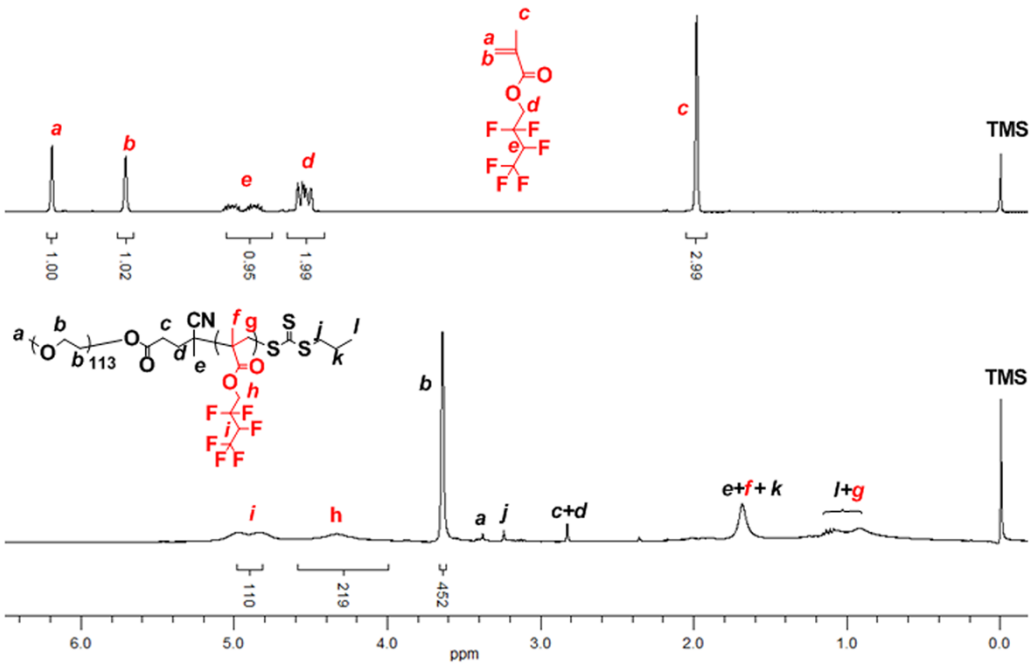

Figure S2. ^{1}H NMR spectra of PEO_{113}–*b*–$PHFBMA_{110}$ diblock copolymers ($O_{113}F_{110}$, bottom) and the HFBMA monomer (top) in $CDCl_3$.

3) Synthesis of the triblock copolymer PEO-*b*-PHFBMA-*b*-PDEAEMA

Using the diblock copolymer $O_{113}F_{110}$ as a macromolecular RAFT agent, the triblock copolymer was synthesized as follows: the diblock copolymer $O_{113}F_{110}$ (1.005 g, ~0.022 mmol), ACPA (1.3 mg, 0.004 mmol), DEAEMA (1.223 g, 6.6 mmol) and 5 mL of 1,4-dioxane were added into a reaction tube equipped with a magnetic bar. Deoxygenizing by three freeze-pump-thaw cycles, the reaction mixture was stored at 70 °C for 48 h with magnetic stirring. The polymerization was terminated by liquid nitrogen. Finally, the product was precipitated in *n*-hexane and lyophilized in a freezing dryer (yield: 1.7 g, conversion: 70%). ^{19}F NMR (δ, ppm, $CDCl_3$; Figure S4): –74 (–C**F**$_3$), –114 (–C**F**$_2$–), –120 (–C**F**–); ^{1}H NMR (δ, ppm, $CDCl_3$; Figure S3): 4.73–5.09 (–C**H**FCF_3), 4.03–4.62 (–COOC**H**$_2$CF_2–), 3.92–4.11 (–COOC**H**$_2$CH_2N(CH_2CH_3)$_2$), 3.63 (–C**H**$_2$C**H**$_2$O–), 3.37 (–OC**H**$_3$), 3.27 (–SC**H**$_2$–), 2.51–2.82 (–OOCC**H**$_2$C**H**$_2$–, –COOCH_2C**H**$_2$N(C**H**$_2$CH_3)$_2$), 1.92–2.11 (–CH_2C**H**$_3$CH_2–), 1.80 (–SCH_2C**H**$_2$CH_3), 0.78–1.30 (–N(C**H**$_2$CH_3)$_2$, –C**H**$_2$CH_3C**H**$_2$–, –SCH_2CH_2C**H**$_3$). From the peak area ratio of PEO_{113} (peak *b* in bottom curve of Figure S3) and the "F" block (peak *i* in bottom curve of Figure S3), it is easy to calculate the polymer degree of DEAEMA, as 212. Then the molecular weight of the triblock copolymer can be calculated as: $M_{n,NMR}$=5276+250×110+185×212=7.2×10^4 g·mol^{-1}; $M_{n,GPC}$=4.03×10^4 g·mol^{-1}, $M_{w,GPC}$=6.47 ×10^4 g·mol^{-1}, M_w/M_n=1.61 (Figure S5).

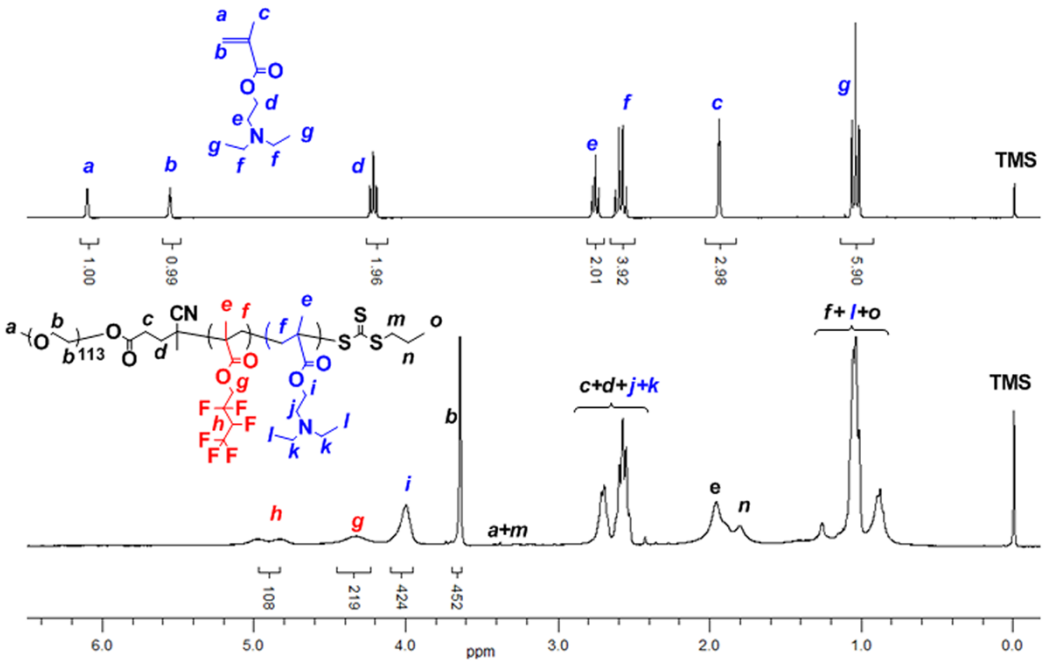

Figure S3. ^{1}H NMR spectra of PEO_{113}–*b*–$PHFBMA_{110}$–*b*–$PDEAEMA_{212}$ triblock copolymer ($O_{113}F_{110}E_{212}$, bottom) and the DEAEMA monomer (top) in $CDCl_3$.

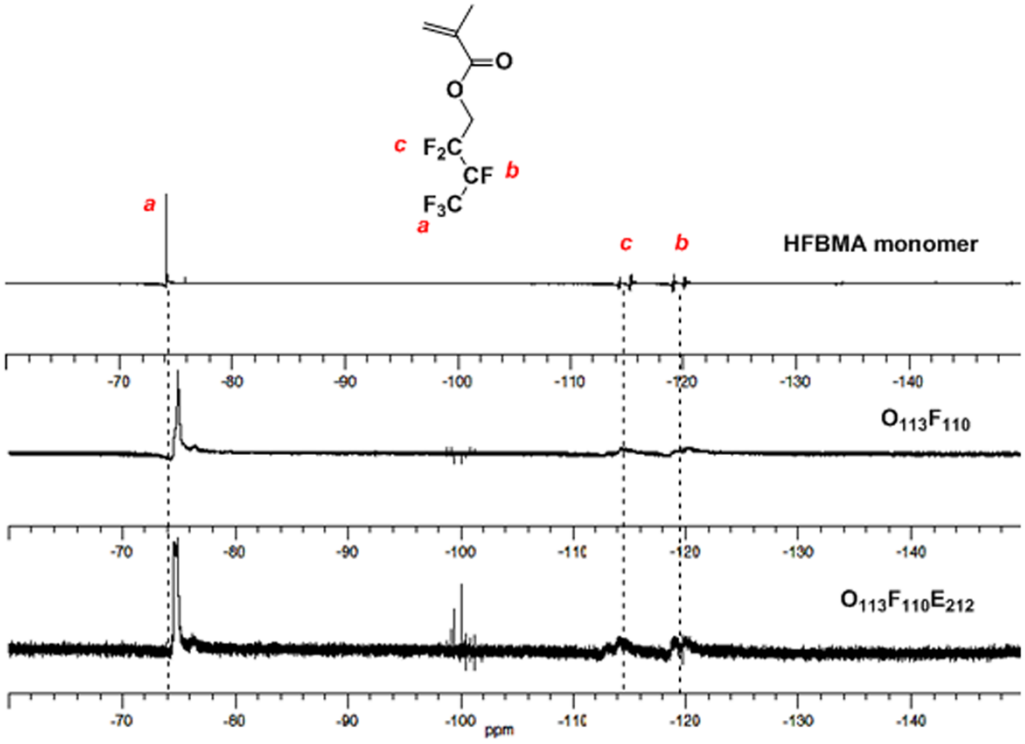

Figure S4. ^{19}F NMR spectra of PEO_{113}–*b*–$PHFBMA_{110}$–*b*–$PDEAEMA_{212}$ triblock copolymer ($O_{113}F_{110}E_{212}$, bottom), PEO_{113}–*b*–$PHFBMA_{110}$ ($O_{113}F_{110}$, middle) and the HFBMA monomer (top) in $CDCl_3$.

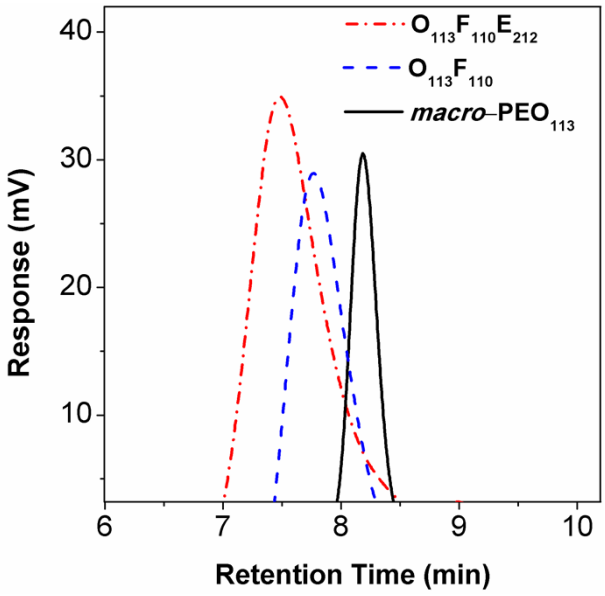

Figure S5 GPC chromatogram for the triblock copolymer PEO_{113}–*b*–$PHFBMA_{110}$–*b*–$PDEAEMA_{212}$ ($O_{113}F_{110}E_{212}$, left), PEO_{113}–*b*–$PHFBMA_{110}$ ($O_{113}F_{110}$, middle) and *macro*-PEO_{113} (right).

4. Preparation of the micelle solutions

15 mg triblock copolymer was dissolved into 5 mL DMF and stirred for more than three hours, and then dialyzed against deionised water. The solution was diluted to 15 mL, so the original micellar solution was obtained with a concentration of 1.0 $g \cdot L^{-1}$. Further experiments involving conductivity, pH, responsiveness to CO_2, TEM and AFM are performed on these original micellar solutions.

In the absence of CO_2, spherical morphology with faint phase separation is obtained (Figure S5a), while typical MCMs are obtained upon exposure to CO_2.

5. Conductivity, pH, pK_a and protonation degree of DEAEMA moities

The conductivity of the triblock copolymer micellar aqueous solution was monitored with a 5 mL original micellar solution by an FE30 conductimeter (Mettler Toledo, USA) at room temperature. The pH variation was monitored with a 5 mL original micellar solution by a Sartorius basic pH-meter PB–10 (± 0.01) calibrated with standard buffer solutions.

The setup for CO_2 bubbling is illustrated in Scheme 2 as follows:

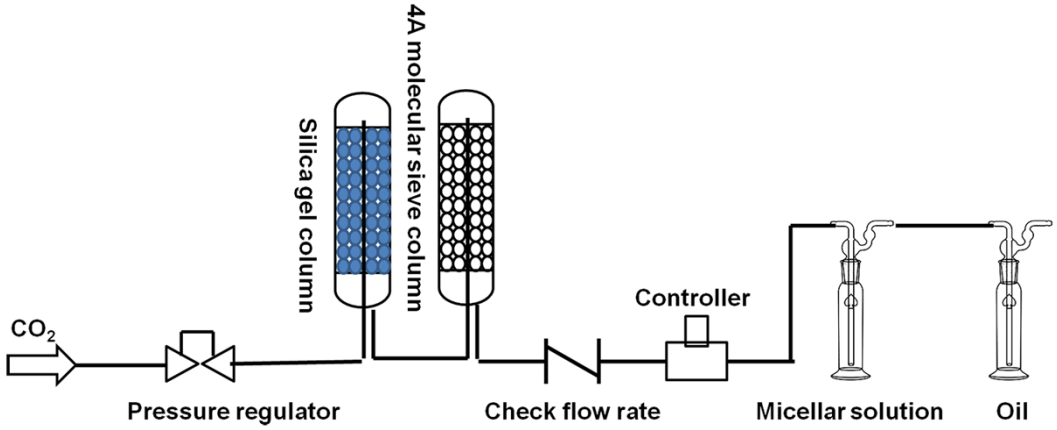

Scheme S2. Schematic diagram of the setup for CO_2 bubbling.

To measure the pK_a of the triblock copolymers in aqueous solution, 5 mL of the original micellar solution was titrated with 20 mM hydrochloric acid calibrated by NaOH, and the pH was continuously monitored. The pH corresponding to the half-equivalence was taken as the average pK_a value,[3] obtained as 5.9 in Figure S6.

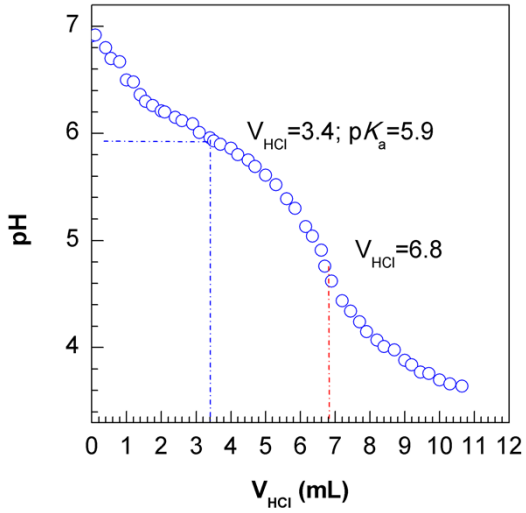

Figure S6. pH titration curve of the triblock copolymer with HCl.

The protonation degree (δ) of PDEAEMA was calculated with the following equations:[3]

$$K_a = \frac{[\text{PDEAEMA}][\text{H}^+]}{[\text{PDEAEMAH}^+]} \quad (1)$$

$$\delta = \frac{[\text{PDEAEMAH}^+]}{[\text{PDEAEMA}]+[\text{PDEAEMAH}^+]} \quad (2)$$

$$\text{pH} = -\log[\text{H}^+] \quad (3)$$

$$\delta = \frac{1}{1+10^{\text{pH-pKa}}} \quad (4)$$

According to the pH values of the triblock copolymer micellar solution measured as a function of CO_2 bubbling time (flow rate fixed at around 15 $mL \cdot min^{-1}$), the protonation degree of the "E" block in $O_{113}F_{110}E_{212}$ at different pH values were calculated and are shown in Table S1. The results show that the protonated degree of the "E" block increases from 2% to 92% when the pH drops from 7.51 to 4.83 in 10 min of CO_2 bubbling, then remains constant in the following 10 min of bubbling CO_2, indicating that the maximal protonation has been reached.

Table S1 Protonation degrees (δ) of E block in $O_{113}F_{110}E_{212}$ at different pH values

Time (min)	0	0.5	1	1.5	2	4	6	10	15	20
pH	7.51	5.57	5.26	5.16	5.10	5.01	4.89	4.83	4.82	4.81
δ (%)	2	68	81	85	86	89	91	92	92	92

6. Cryo-TEM observation

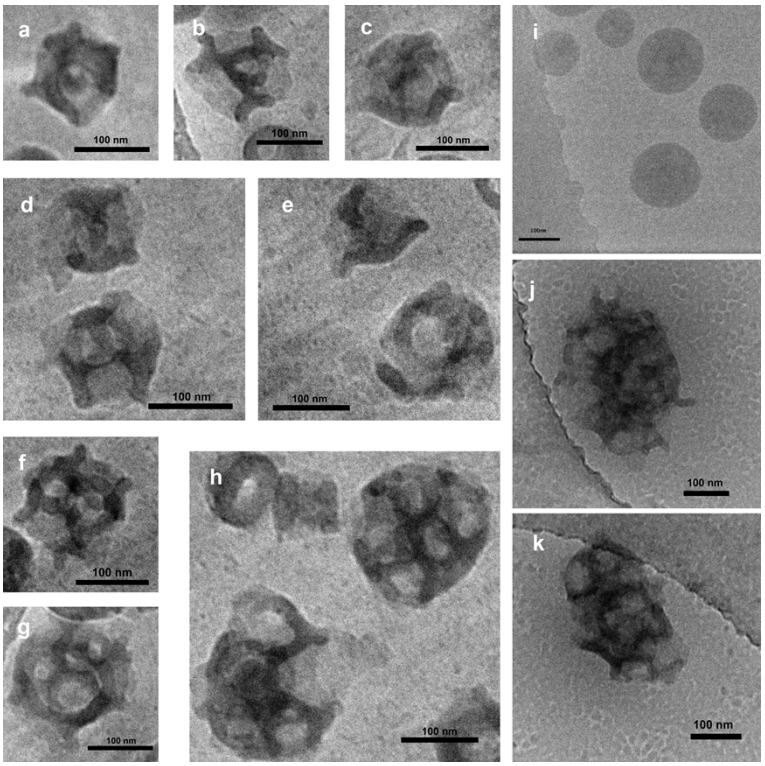

Figure S7. Cryo-TEM images of micelles of triblock copolymer $O_{113}F_{110}E_{212}$ after bubbling CO_2 (a–h), removing CO_2 by bubbling N_2 (i), and re-bubbling CO_2 (j and k). The samples are free of staining. Bars: 100 nm.

7. SEM observation

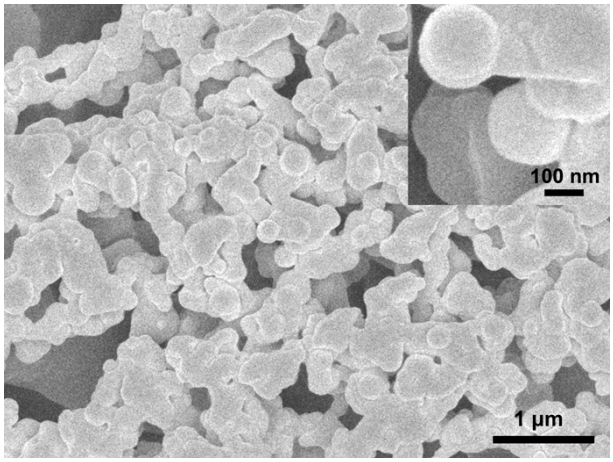

Figure S8 SEM image of triblock copolymer $O_{113}F_{110}E_{212}$ after bubbling CO_2

8. Thermal behaviour

The thermal behaviour of the ABC triblock copolymer $O_{113}F_{110}E_{212}$ was examined with differential scanning calorimetry (DSC) under nitrogen atmosphere from –80 to 100 °C with a heating rate of 10 °C·min^{-1}. To distinguish the endothermic peaks from the "E" and "F" blocks, two diblock copolymer precursors, PEO_{113}-*b*-$PDEAEMA_{212}$ ($O_{113}E_{212}$) and PEO_{113}-*b*-$PHFBMA_{110}$ ($O_{113}F_{110}$), were measured for comparison.

All block copolymers exhibit endothermic peaks at −70°C and 50°C, corresponding to the glass transition temperature (T_g) and melting point (T_m), respectively, of PEO (Figure S9, left).[4] Both triblock copolymer $O_{113}F_{110}E_{212}$ and diblock $O_{113}E_{212}$ precursor show a wide endothermic peak at around 30–45 °C (Figure S9, right),[5] attributed to the T_g of the E block. In addition, the triblock $O_{113}F_{110}E_{212}$ also exhibits a T_g at 68 °C, corresponding to the F block, close to that of $O_{113}F_{110}$ (62 °C). [6] The independent T_g of the hydrocarbon "E" block and fluorocarbon "F" block, may suggest that the blocks F and E are phase-separated. Nevertheless, an additional peak at 85 °C arises in the DCS curve of the triblock copolymer $O_{113}F_{110}E_{212}$, indicating the coexistence of three microphases of each polymer block.[7] This means that the macro-phase separation is incomplete when the "E" block is in the hydrophobic state before reaction with or after removal of CO_2.

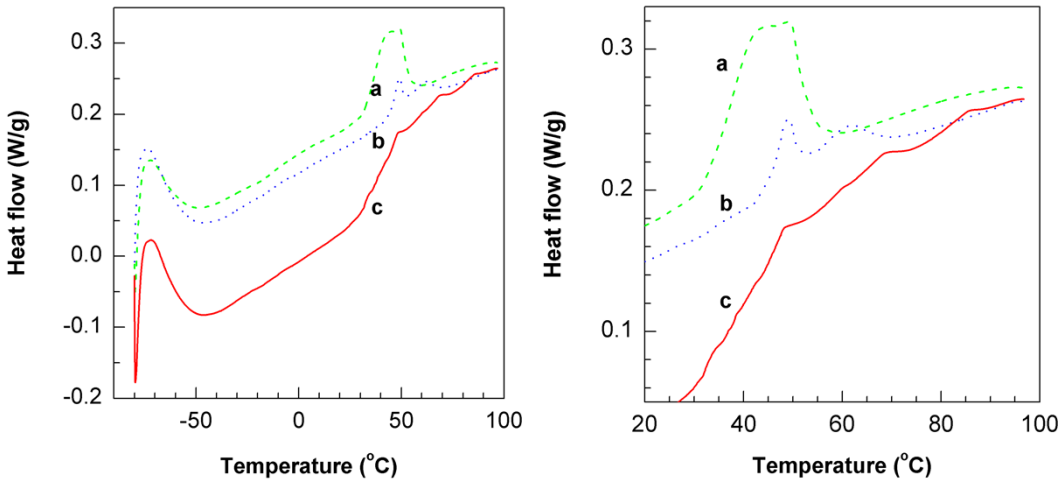

Figure S9. Left-hand side: DSC trace of the bulk copolymers (a: $O_{113}E_{212}$, b: $O_{113}F_{110}$, c: $O_{113}F_{110}E_{212}$). Right-hand side: close-up on the temperature range from 20 to 100°C.

9. Dissipative particle dynamics (DPD) simulation

In addition to the visualization of MCMs with TEM and cryo-TEM, a dissipative particle dynamics (DPD) simulation on the self-assemblies before and after treatment with CO_2 was performed to confirm MCM formation. The computer simulation results support the experimental observations, theoretically demonstrating the formation of MCMs after reaction with CO_2. The simulation and related discussion about the results are presented below:

1) Dissipative Particle Dynamic Method

DPD is a mesoscopic simulation technique introduced by Hoogerbrugge and Koelman in 1992.[8] A DPD bead represents a group of atoms or a volume of fluid that is large on the atomistic scale but still macroscopically small.[9] The force experienced by particle i is composed of three parts: a conservative force F^C, a dissipative force F^D, and a random force F^R. To model the block copolymers, we tie the adjacent beads in a single polymer chain by harmonic spring force F^S. Each force is additive pairwise:

$$\mathrm{F}_i = \sum_{j \neq i} (\mathrm{F}_{ij}^C + \mathrm{F}_{ij}^D + \mathrm{F}_{ij}^R + \mathrm{F}_{ij}^S) . \quad (5)$$

The sum runs over all other particles within a cutoff radius r_c. The different components of the forces are given by:

$$\mathrm{F}_{ij}^C = -\alpha_{ij}\omega^C(r_{ij})\mathrm{e}_{ij}, \quad (6)$$

$$\mathrm{F}_{ij}^D = -\gamma\omega^D(r_{ij})(\mathrm{v}_{ij}\cdot\mathrm{e}_{ij})\mathrm{e}_{ij}, \quad (7)$$

$$\mathrm{F}_{ij}^R = \sigma\omega^R(\mathrm{r}_{ij})\xi_{ij}\Delta t^{-1/2}\mathrm{e}_{ij}, \quad (8)$$

$$\mathrm{F}_{\mathrm{ij}}^S = Cr_{ij}, \quad (9)$$

where $\mathrm{r}_{ij} = \mathrm{r}_i - \mathrm{r}_j$, $r_{ij} = \left|\mathrm{r}_{ij}\right|$, $\mathrm{e}_{ij} = \mathrm{r}_{ij}/r_{ij}$, r_i and r_j are the positions of particle *i* and particle *j*, respectively. $\mathrm{v}_{ij} = \mathrm{v}_i - \mathrm{v}_j$, v_i and v_j are the velocities of particle *i* and particle *j*, respectively. α_{ij} is a constant which describes the maximum repulsion between interacting beads. γ and σ are the amplitudes of dissipative and random forces, respectively. ω^C, ω^D, and ω^R are three weight functions for the conservative, dissipative, and random forces, respectively. For the conservative force, we choose $\omega^C(r_{ij}) = 1 - r_{ij}/R_c$ for $r_{ij} < R_c$ and $\omega^C(r_{ij}) = 0$ for $r_{ij} \geq R_c$, $\omega^D(r_{ij})$ and $\omega^R(r_{ij})$ follow a certain relation according to the fluctuation-dissipation theorem,[10]

$$\omega^D(r) = \left[\omega^R(r)\right]^2, \sigma^2 = 2\gamma\kappa_B T. \qquad (10)$$

Here we choose a simple form of ω^D and ω^R following Groot and Warren,[9]

$$\omega^D(r) = \left[\omega^R(r)\right]^2 \begin{cases} (1 - r/R_C)^2 (r < R_C) \\ 0 (r \geq R_C) \end{cases} \qquad (11)$$

ξ_{ij} is a random number with zero mean and unit variance, chosen independently for each interacting pair of beads at each time step Δt. A modified version of velocity-Verlet algorithm[9] is used here to integrate the equations of motion. For easy numerical handling, we have chosen the cutoff radius, the particle mass, and the temperature as the units of the simulated system, i.e., $R_C = m = K_B T = 1$. As a consequence, the unit of time τ is $\tau = R_C\sqrt{m/K_B T} = 1$.

The conservative interaction strength α_{ij} is chosen according to the linear relation with the Flory-Huggins χ parameters as

$$\alpha_{ij} = \alpha_{ii} + 3.27\chi_{ij} \qquad (\rho = 3). \qquad (12)$$

where the interaction parameter between the same type of bead α_{ii} equals 25 to correctly describe the compressibility of water,[9] and $\rho = 3$ is the number density in our simulations. The spring constant C is set to 4.0, which is enough to keep the adjacent beads connected together along the polymer backbone.[11]

2) Understanding Multicompartment Micelles Using DPD Simulation

Zhong and co-workers[12–15] have determined the DPD repulsion parameters between unlike species of ABC block copolymer, consisting of the weakly hydrophobic poly(ethylethylene), the hydrophilic poly(ethylene oxide), and the strongly hydrophobic poly(perfluoropropylene oxide), which is successfully used to study the experimental work of Lodge and co-workers.[16] A systematic DPD study has also been successfully performed by Zhao et al[15,17–18] to study the self-assembly of block copolymers in aqueous solution.

In order to better understand the CO_2-responsive MCMs with segregated corona made from a linear triblock copolymer based on hydrophilic poly(ethylene oxide) (O), strongly hydrophobic poly(2,2,3,4,4,4-hexafluorobutyl methacrylate) (F), and weakly hydrophobic poly(2-diethylamino)ethyl methacrylate) (E), one model ABC linear triblock copolymer $A_{12}B_6C_{10}$ was constructed to mimic the linear triblock copolymer $O_{113}F_{110}E_{212}$ studied in the experiment. In this work, the water molecule (W) is modeled as a single DPD bead, and the linear triblock copolymers $A_{12}B_6C_{10}$ are modeled by connected DPD beads. Various sets of DPD parameters were examined, and the sets shown in Table S2 and Table S3 enabled the constructed copolymers to reproduce the morphologies of the triblock copolymer assemblies in water observed for (a) before bubbling CO_2 and (b) after bubbling CO_2 in the experiment, respectively.

Furthermore, the simulations are performed in a cubic cell of size $40\times40\times40\,r_c^3$. The total volume fraction of linear triblock copolymers is 0.10 to guarantee dilute conditions. Periodic boundary conditions are applied. The time step Δt is taken as 0.05, and 6×10^5 DPD time steps are carried out to attain equilibration for each system.

Table S2 DPD repulsion parameter α_{ij} (in DPD units) used in the simulation of self-assembly of the ABC linear triblock copolymers in water before bubbling CO_2

	W	A	B	C
W	25	27	120	50
A	27	25	90	45
B	120	90	25	30
C	50	45	30	25

Table S3 DPD repulsion parameter α_{ij} (in DPD units) used in the simulation of self-assembly of the ABC linear triblock copolymers in water after bubbling CO_2

	W	A	B	C
W	25	27	120	50
A	27	25	90	45
B	120	90	25	75
C	50	45	75	25

3) Results and Discussion

The linear triblock copolymer $A_{12}B_6C_{10}$ self-assembles into spherical micelles in water before bubbling CO_2, in which the hydrophilic block A (block O) forms the shell, and the hydrophobic block B and block C form the core of the micelles, as shown in Figures S10a and S10b. However, due to the weak interaction between the hydrophobic block B (block F) and block C (block E), the phase separation is incomplete (Figure S10a–c); this can be observed from the cross-section of the micelle shown in Figure S10d.

After treatment with CO_2, the pendant tertiary amine groups in the "E" block become protonated (from 2% to 92%), which corresponds to higher interaction force between block B and block C. The repulsion parameter α_{BC} changes from 30 (before bubbling CO_2) to 75 (after bubbling CO_2). The morphology of multicompartment micelles with distinct segregated micro-domains is observed and shown in Figure 4 after bubbling of CO_2.

These simulations thus confirm the structure of MCMs with a segregated corona, which can reversibly be switched "on" and "off" by alternately bubbling and displacing CO_2,

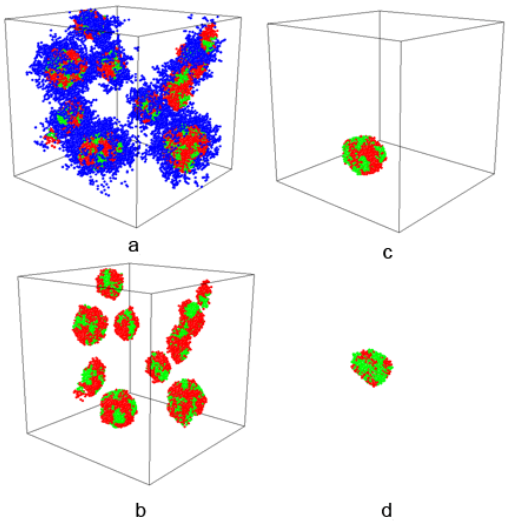

Fig. S10 Morphologies of the triblock copolymer self-assembly in water before bubbling CO_2 (a): triblock copolymer $A_{12}B_6C_{10}$ self-assembly in water, block A: blue, block B: red, block C: green; (b) self-assembly of the core of the triblock copolymer $A_{12}B_6C_{10}$; (c) core of one micelle; (d) cross-section of the core of the micelle.

References

1. X. W. Xu, A. E. Smith, S. E. Kirkland, C. L. McCormick, *Macromolecules*, 2008, **41**, 8429–8435.
2. A. J. Convertine, D. S. W. Benoit, C. L. Duvall, A. S. Hoffman, P. S. Stayton, *J. Control. Release*, 2009, **133**, 221–229.
3. B. Yan, D. H. Han, O. Boissiere, P. Ayotte, Y. Zhao, *Soft Matter*, 2013, **9**, 2011–2016.
4. C. W. Walker, M. Salomon, *J. Electrochem. Soc.*, 1993, **140**, 3409–3412.
5. A. Canul-Chuil, R. Vargas-Coronado, J. V. Cauich-Rodríguez, A. Martínez-Richa, E. Fernandez, S.N. Nazhat, *J. Biomed. Mater. Res. Part B: Appl. Biomater.*, 2003, **64B**, 27–37.

6. J. J. Wang, Y. N. Zhou, P. Wang, Z. H. Luo, *RSC Adv.*, 2013, **3**, 5045–5055.
7. K. Skrabania, A. Laschewsky, H. von Berlepsch, C. Bottcher, *Langmuir*, 2009, **25**, 7594–7601.
8. P. J. Hoogerbrugge, J. M. V. A. Koelman, *Europhys. Lett.*, 1992, **19,** 155–160.
9. R. D. Groot, P. B. Warren, *J. Chem. Phys.*, 1997, **107**, 4423–4435.
10. P. Español, P. W. Warren, *Euro. Phys. Lett.*, 1995, **30**, 191–196.
11. R. D. Groot, T. J. Madden, *J. Chem. Phys.*, 1998 **108**, 8713–8723.
12. C. Zhong, D. Liu, *Macromol. Theory Simul.*, 2007, **16**, 141–157.
13. D. Liu, C. Zhong, *Polymer*, 2008, **49** 1407–1413.
14. J. Xia, D. Liu, C. Zhong, *Phys. Chem. Chem. Phys.*, 2007 **9**, 5267–5273.
15. Y. Zhao, Y. Liu, Z. Lu, C. Sun, *Polymer*, 2008, **49** 4899–4909.
16. Z. Li, E. Kesselman, Y. Talmon, M. A. Hillmyer, T. P. Lodge, *Science*, 2004, **306**, 98–101.
17. Y. Zhao, L. You, Z. Lu, C. Sun, *Polymer*, 2009 **50**, 5333–5340.
18. B. Xu, Y. Zhao, X. Shen, Y. Cong, X. Yin, X. Wang, Q. Yuan, N. Yu, B. Dong, *Acta Phys.-Chim. Sin.* , 2014, **30**, 646–653.